Thermochimica Acta, 67 (1983) 271–285
Elsevier Science Publishers B.V., Amsterdam – Printed in The Netherlands

THERMAL DECOMPOSITION OF FORMATES. PART IX. THERMAL DECOMPOSITION OF RARE EARTH FORMATE ANHYDRIDES

YOSHIO MASUDA

Division of Chemistry, General Education Department, Niigata University, Niigata 950-21 (Japan)

(Received 4 March 1983)

ABSTRACT

The thermal decomposition of rare earth formate anhydrides in a flowing nitrogen atmosphere was studied systematically by means of thermogravimetry and differential thermal analysis.

The decomposition consisted of two or three stages

$$2\ Ln(HCO_2)_3 \rightarrow 2\ LnO(HCO_2) \rightarrow Ln_2O_2 \cdot CO_3 \rightarrow Ln_2O_3$$

The monoxyformate did not appear in the decomposition of the lighter element formates except for lanthanum formate. The oxycarbonate was observed across the series. The crystal structure of oxycarbonate for praseodymium and neodymium was monoclinic-type and that for the other elements was tetragonal-type.

The thermal stability of rare earth formates was related to their structural distortion which must be attributed to the contraction of the radii of rare earth metallic ions.

The first stage of decomposition for lanthanum to dysprosium formate was the Avrami-type reaction. The formates of holmium to lutetium melted during the main first stage of decomposition and their kinetics were characteristic of a first-order reaction.

The kinetic parameters, such as activation energy and pre-exponential factor, were determined for the main stage of the decomposition.

INTRODUCTION

Although many investigations have been carried out on the thermal decomposition of rare earth metal formates, their thermal behaviour has not been satisfactorily elucidated. In addition, many kinds of intermediates formed during the decomposition have been reported. Ambroghii and Osipova [1] have studied the decomposition of some rare earth formates and found $Ln_2O_3 \cdot 6\ CO$ as an intermediate. Plyushchev et al. [2,3] have suggested that the rare earth formates decomposed through $Ln_2(CO_3)_3$ to Ln_2O_3. Turcotte et al. [4] have also studied the decomposition of some rare earth formates in a carbon dioxide atmosphere and showed that their decomposition consisted of

$$Ln(HCO_2)_3 \rightarrow LnO(HCO) \rightarrow Ln_2O_2 \cdot CO_3 \rightarrow Ln_2O_3$$

0040-6031/83/$03.00

They also suggested the formation of intermediates, i.e. monoxytetraformate, $Ln_2O(HCO_2)_4$, for lanthanum and praseodymium formates and the pentoxymonocarbonate, $Ln_4O_5 \cdot CO_3$, for ytterbium and lutetium formates. Kavedia and Mathur [5] have suggested that the decomposition of rare earth formates in a flowing air atmosphere consisted of

$$Ln(HCO_2)_3 \rightarrow Ln_2O \cdot (CO_3)_2 \rightarrow Ln_2O_2 \cdot CO_3 \rightarrow Ln_2O_3$$

Taylor and Panayappan [6] reported that some rare earth formates decompose through $Ln_2O_2 \cdot CO_3$. Dabkowska [7,8] has also examined the thermal decomposition of europium, terbium and lutetium formates and suggested the formation of intermediates, $EuCO_3$ and $Lu_2O \cdot (CO_3)_2$. However, these intermediates have not been characterized satisfactorily.

In this paper, the thermal decomposition reactions of rare earth metal formate anhydrides in a flowing nitrogen atmosphere are studied systematically and the stoichiometry of the thermal reaction is re-examined. In addition, the kinetics of their main decomposition stage is discussed and the influence of the lanthanoid contraction of the metallic ion on the thermal behaviour of these compounds is also discussed.

EXPERIMENTAL

Materials

All the formates were prepared by the reaction of formic acid and rare earth metal oxides (99.9%) which were purchased from Mitswa Pure Chemical Co., Osaka, Japan.

The formates of La, Ce, Pr, Nd, Sm, Eu, Gd and Tb crystallized as anhydrides, while the formates of Dy, Ho, Er, Tm, Yb and Lu were separated as dihydrates. The results of elemental analyses for C, H and metal are shown in Table 1.

Measurements

Each sample was pulverized in a mortar with a pestle and sieved to narrow fraction of 250–300 mesh size in order to carry out the decomposition process under the same conditions for all the salts.

TG and DTA curves were obtained simultaneously with a Rigaku Thermoflex TG-DTA M 8075 at a heating rate of 5 K min^{-1}, in a flowing nitrogen atmosphere (flow rate: 90 cm^3 min^{-1}). About 10 mg of sample were weighed into a platinum crucible and measured using α-alumina as a reference material.

Isothermal TG curves were obtained with a Shinku Riko TGD-3000 thermal microbalance.

TABLE 1

Analytical data of the rare earth formates, $Ln(HCO_2)_3$

Ln	C		H		M [a]	
	Obsd. (%)	Calcd. (%)	Obsd. (%)	Calcd. (%)	Obsd. (%)	Calcd. (%)
La	12.66	13.14	1.23	1.10	49.04	50.88
Ce	13.08	12.50	1.14	1.09	51.03	50.93
Pr	12.97	13.05	1.13	1.09	50.05	51.07
Nd	12.70	12.95	1.17	1.08	51.13	51.65
Sm	12.32	12.61	1.07	1.05	52.76	52.69
Eu	12.44	12.54	1.11	1.05	52.27	52.96
Gd	12.20	12.31	1.02	1.03	53.59	53.81
Tb	12.22	12.24	1.02	1.02	53.97	54.07
Dy [b]	10.53	10.71	2.20	2.10	49.45	48.72
Ho [b]	10.54	10.71	2.09	2.08	48.99	49.09
Er [b]	10.39	10.64	2.11	2.09	48.87	49.44
Tm [b]	10.65	10.59	2.15	2.06	50.37	49.69
Yb [b]	10.61	10.47	2.07	2.03	51.01	50.30
Lu [b]	10.63	10.40	2.08	2.02	50.87	50.57

[a] The metal content was determined by titration with EDTA and xylenol orange.
[b] Calculated for $Ln(HCO_2)_3 \cdot 2\ H_2O$.

Infrared absorption (IR) spectra of samples heated to various temperatures were measured from 250 to 4000 cm^{-1} in a KBr disc using a Hitachi 295 spectrophotometer.

X-Ray powder diffraction analysis was made using a Rigaku Geigerflex diffractometer.

Evolved gaseous products of decomposition were collected in syringes at intervals of 2 min from 423 to 1000 K, and 2 cm^3 of each gas collected were analyzed with a Shimadzu GC-3BT gas chromatograph [9]. The separation columns were 2.0 m × 3 mm I.D. and 1.5 m × 3 mm I.D. stainless-steel, packed with molecular sieve 5A (60–80 mesh) and silica gel (60–80 mesh), respectively. The column temperature was 343 K, and nitrogen and hydrogen were used as the carrier gas at a flow rate of 60 $cm^3\ min^{-1}$.

RESULTS AND DISCUSSION

TG and DTA curves of $Ln(HCO_2)_3$ in a flowing nitrogen atmosphere are shown in Fig. 1. These curves showed an interesting tendency in that the decomposition of the anhydrous rare earth formates was simpler than that of the dihydrated formates.

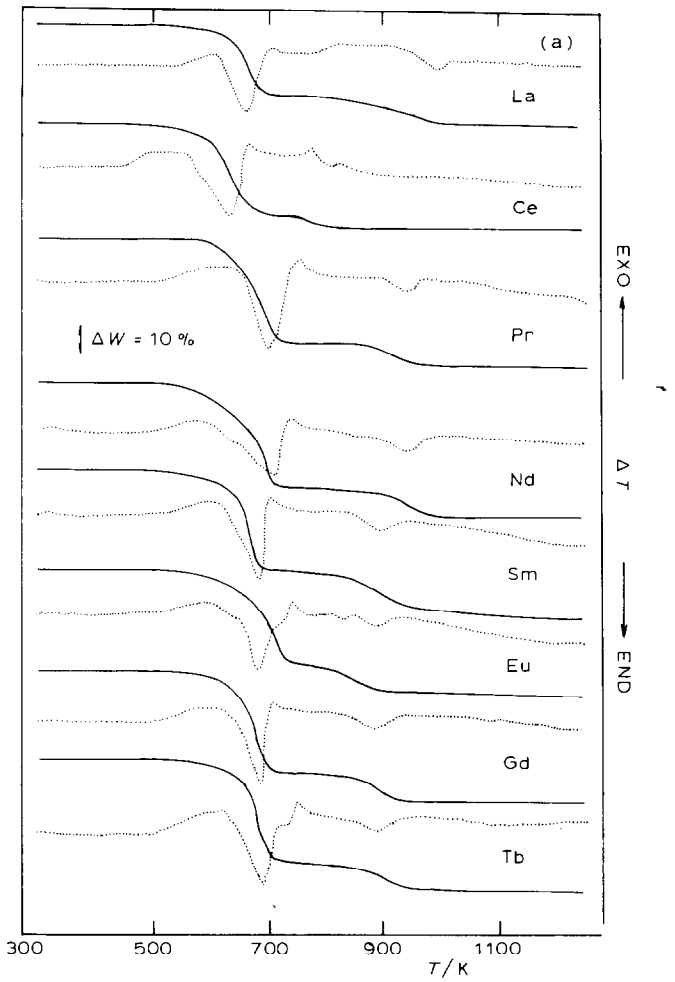

Fig. 1.(a) TG (solid line) and DTA (broken line) curves for the thermal decomposition of rare earth formates in a nitrogen atmosphere (heating rate 5 K min^{-1}).

Thermal decomposition of anhydrous rare earth formates of La, Ce, Pr, Nd, Sm, Eu, Gd and Tb

TG curves of these compounds show that their decomposition proceeds through at least two stages [Table 2].

The first stage of the $La(HCO_2)_3$ decomposition occurred in the temperature range 543–683 K and, corresponding to the weight loss, an endothermic peak was recognized at 645 K. The weight loss associated with this process, 30.82%, is less than that expected, 32.49%, for the decomposition of $La(HCO_2)_3$ to $La_2O_2 \cdot CO_3$. This discrepancy suggested that the decomposition was incomplete at this temperature and another intermediate must be formed.

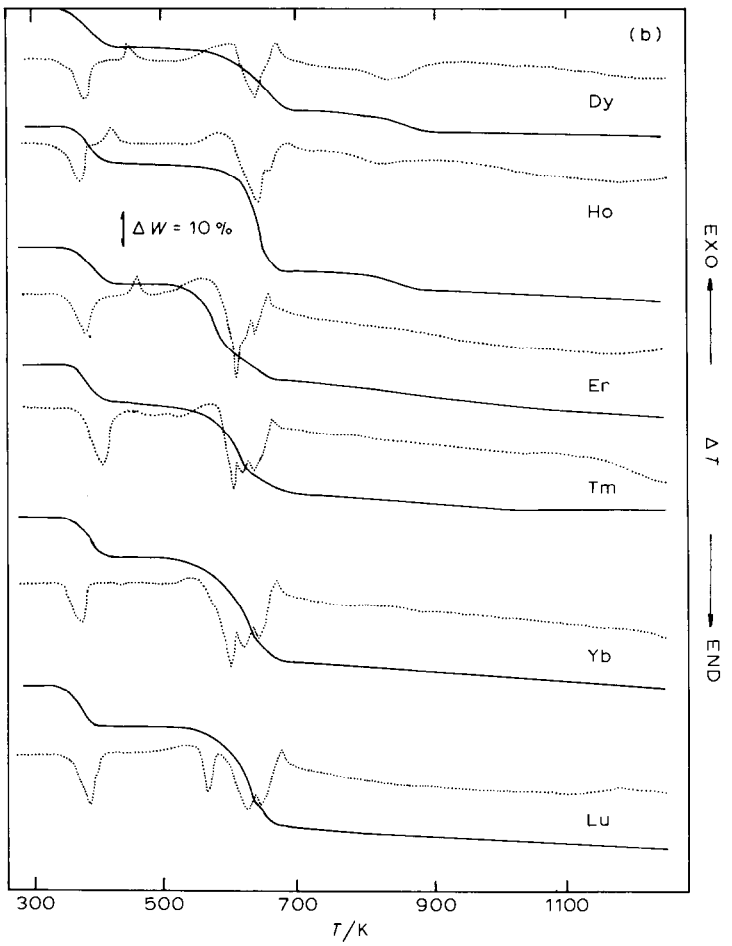

Fig. 1.(b) TG (solid line) and DTA (broken line) for the thermal decomposition of rare earth formates in a nitrogen atmosphere (heating rate 5 K min^{-1}).

Gas analysis showed that the decomposition involved almost simultaneous evolution of H_2 and CO_2 at 543 K, and CO at 613 K (Fig. 2). The lag in the appearance of CO seems to be due to the disproportionation of CO which caused a slight and broad exotherm observed at around 623 K. The composition of the gaseous products at this stage was H_2, 33.7%; CO, 32.7% and CO_2, 33.7%.

The residue at this stage was poorly crystalline and its IR spectrum resembled that of $La_2O_2 \cdot CO_3$. However, the broad band observed at around 2900 cm^{-1} which was assigned to C–H stretching and the shoulder observed at around 1580 cm^{-1} which was assigned to CO asymmetric stretching showed the presence of the HCO_2 group [10–16]. From these experimental results, the residue seems to be a mixture of $La_2O_2 \cdot CO_3$ and $LaO(HCO_2)$.

TABLE 2

Thermal analysis data of rare earth formate anhydrides, $Ln(HCO_2)_3$, in a flowing nitrogen atmosphere

Ln	Stage of decomp.	Temp. range (K)	T_p [a] (K)	Weight loss		Solid product	Evolved gas (%)
				Obsd. (%)	Calcd. (%)		
La	1	543– 683	645	30.82	32.49	$LaO(HCO_2)$ $La_2O_2 \cdot CO_3$ C	H_2(23.2) CO(24.2) CO_2(27.1)
	2	683–1043	773– 873 963	9.45	8.03	La_2O_3, C	H_2(12.0) CO_2(13.5)
Ce	1	453– 663	642	31.65	32.35	$Ce_2O_2 \cdot CO_3$ C	H_2(36.1) CO(19.4) CO_2(30.7)
	2	663– 973		7.45	8.00	Ce_2O_3	CO_2(13.8)
Pr	1	543– 713	698	31.98	32.26	$Pr_2O_2 \cdot CO_3$ C	H_2(35.4) CO(23.1) CO_2(28.4)
	2	773– 973		8.33	7.97	Pr_2O_3	CO_2(13.1)
Nd	1	543– 703	671	31.03	31.88	$Nd_2O_2 \cdot CO_3$ C	H_2(35.6) CO(22.2) CO_2(29.2)
	2	813– 953	936	8.08	7.88	Nd_2O_3	CO_2(13.0)
Sm	1	533– 693	678	31.03	31.19	$Sm_2O_2 \cdot CO_3$ C	H_2(35.8) CO(21.3) CO_2(29.4)
	2	693– 973	893	7.60	7.71	Sm_2O_3	CO_2(13.0)
Eu	1	537– 725	687	30.84	31.02	$Eu_2O_2 \cdot CO_3$ C	H_2(35.9) CO(20.7) CO_2(29.7)
	2	725– 913	863	7.89	7.66	Eu_2O_3	CO_2(13.7)
Gd	1	543– 693	683	30.50	30.45	$Gd_2O_2 \cdot CO_3$ C	H_2(35.8) CO(21.1) CO_2(29.1)
	2	773– 933	883	7.73	7.53	Gd_2O_3	CO_2(14.0)
Tb	1	543– 688	675	24.10	25.18	$TbO(HCO_2)$ C	H_2(25.5) CO(10.9) CO_2(25.2)
	2	688– 703		5.10	5.10	$Tb_2O_2 \cdot CO_3$ C	H_2(10.5) CO(9.1) CO_2(5.1)
	3	703– 973	853	7.37	7.49	Tb_2O_3	CO_2(13.7)
Dy	1	513– 673	648	29.11	29.92	$Dy_2O_2 \cdot CO_3$ C	H_2(35.6) CO(22.2) CO_2(27.4)
	2	673–1053	784	7.39	7.40	Dy_2O_3	CO_2(14.8)

TABLE 2 (continued)

Ln	Stage of decomp.	Temp. stage (K)	T_p [a] (K)	Weight loss		Solid product	Evolved gas (%)
				Obsd. (%)	Calcd. (%)		
Ho	1	513– 648	642	24.05	24.67	$HoO(HCO_2)$ C	H_2(22.9) CO(15.1) CO_2(22.1)
	2	648– 663	647	5.34	5.00	$Ho_2O_2 \cdot CO_3$ C	H_2(11.8) CO(11.9) CO_2(3.4)
	3	663– 973	823	7.13	7.33	Ho_2O_3	CO_2(12.8)
Er	1	515– 623	593	24.00	24.48	$ErO(HCO_2)$ C	H_2(25.2) CO(16.0) CO_2(24.9)
	2	623– 643	625	5.00	4.96	$Er_2O_2 \cdot CO_3$ C	H_2(9.7) CO(9.3) CO_2(3.1)
	3	643–1153		7.50	7.28	Er_2O_3	CO_2(11.8)
Tm	1	483– 633	605 615	24.59	24.03	$TmO(HCO_2)$ C	H_2(23.4) CO(16.6) CO_2(23.5)
	2	633– 693	636	4.05	4.93	$Tm_2O_2 \cdot CO_3$ C	H_2(11.0) CO(11.1) CO_2(2.5)
	3	693–1173		6.97	7.24	Tm_2O_3	CO_2(11.9)
Yb	1	473– 628	603 621	24.59	24.03	$YbO(HCO_2)$ C	H_2(22.9) CO(19.9) CO_2(21.7)
	2	628– 653	634	5.16	4.87	$Tm_2O_2 \cdot CO_3$	H_2(11.0) CO(10.7) CO_2(2.5)
	3	653–1233		7.62	7.14	Yb_2O_3	CO_2(11.3)
Lu	1	473– 635	571 625	23.82	23.87	$LuO(HCO_2)$ C	H_2(22.1) CO(20.2) CO_2(24.3)
	2	635– 653	641	5.21	4.86	$Lu_2O_2 \cdot CO_3$ C	H_2(11.2) CO(10.2) CO_2(2.4)
	3	723–1133		6.95	7.10	Lu_2O_3	CO_2(10.2)

[a] Peak temperature of DTA curve.

The formation of $LaO(HCO_2)$ has not been reported for the decomposition of $La(HCO_2)_3$ in a nitrogen atmosphere, but it has been confirmed by Turcotte et al. in a carbon dioxide atmosphere [4].

The weight ratio of $La_2O_2 \cdot CO_3 : LaO(HCO_2)$ estimated from the weight-loss value was 2.2 : 1.0.

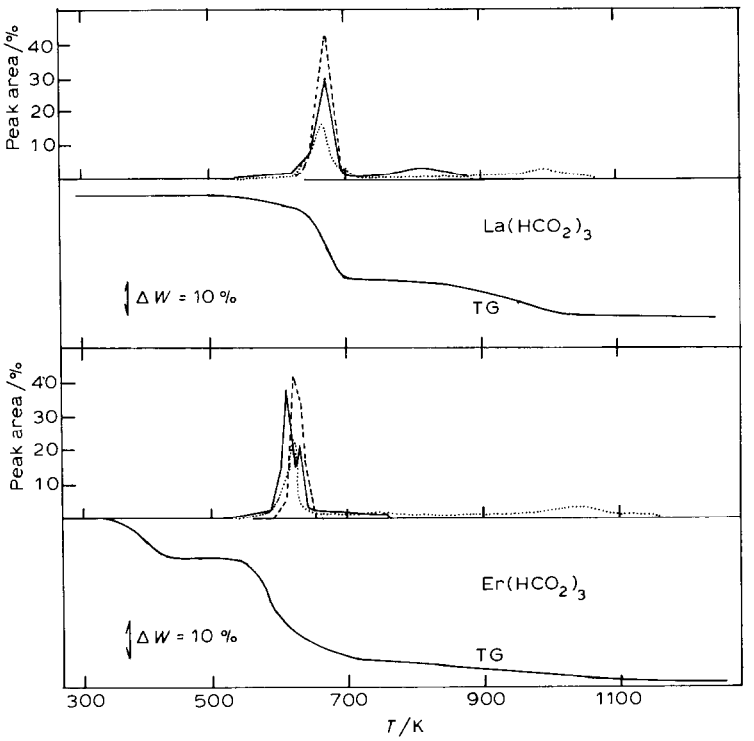

Fig. 2. Evolved H_2 (————), CO (- - - - - -) and CO_2 (· · · · · ·) on the thermal decomposition of $La(HCO_2)_3$ and $Er(HCO_2)_3$ in a nitrogen atmosphere.

The second stage occurred successively and appeared to be complete at 1043 K. Corresponding with this process, two endotherms were observed. The former, which was very weak and broad, was found in the temperature range 733–870 K, and the latter at 963 K. This result suggests that the second stage consists of at least two processes.

The IR spectrum of the sample heated to 700 K showed a weak C–H stretching band at around 2900 cm^{-1}, but this band was no longer detectable for the sample heated to 873 K. Therefore, the former and weak endotherm must correspond to the reaction

$$2\ LaO(HCO_2) \rightarrow La_2O_2 \cdot CO_3 + H_2 + CO \quad (1)$$

and the latter one to

$$La_2O_2 \cdot CO_3 \rightarrow La_2O_3 + CO_2 \quad (2)$$

which took place continuously in the temperature range 873–1043 K.

The grey colour of the residue which was due to the dispersed carbon showed the disproportionation of carbon monoxide formed in reaction (1).

The ratio of H_2 evolved in the first stage to that in the second stage was 9 : 1, which indicated that about 30% of $La(HCO_2)_3$ was converted to

$LaO(HCO_2)$ in the first stage. This result is not contradictory to that estimated from the weight-loss value. The total weight loss for the second stage, 9.45%, which was the mixture of those of reactions (1) and (2), was in agreement with the expected value, 9.67%.

It has been known that there are three polymorphic forms of the oxycarbonate of rare earth metals, namely, tetragonal (type I), monoclinic (type IA) and hexagonal (type II) [17]. The oxycarbonate, $La_2O_2 \cdot CO_3$ formed in this decomposition was type I, as identified by its IR spectrum.

The thermal decompositions of Ce, Pr, Nd, Sm, Eu and Gd formates are similar to each other and the results are summarized in Table 2. Their decomposition consisted of two distinct stages

$$2\ Ln(HCO_2)_3 \rightarrow Ln_2O_2 \cdot CO_3 + 3\ H_2 + 3\ CO + 2\ CO_2$$

$$Ln_2O_2 \cdot CO_3 \rightarrow Ln_2O_3 + CO_2$$

The oxyformate formed was type IA for praseodymium and neodymium formates, and type I for the other formates (Fig. 3) [17].

The decomposition of terbium formate took place in three stages

$$Tb(HCO_2)_3 \rightarrow TbO(HCO_2) + H_2 + CO_2 + CO$$

$$2\ TbO(HCO_2) \rightarrow Tb_2O_2 \cdot CO_3 + H_2 + CO$$

$$Tb_2O_2 \cdot CO_3 \rightarrow Tb_2O_3 + CO_2$$

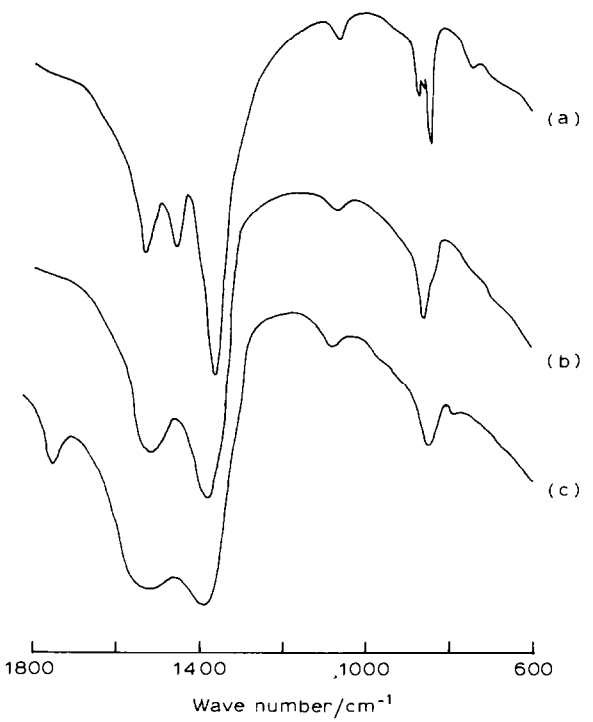

Fig. 3. IR spectra of oxycarbonates, $Ln_2O_2 \cdot CO_3$. (a) $Pr(HCO_2)_3$ heated to 773 K, type IA; (b) $Eu(HCO_2)_3$ heated to 850 K, type I; (c) $Yb(HCO_2)_3$ heated to 673 K, type I.

An endothermic peak, which had a shoulder at the high temperature side, was observed at 675 K. The peak and shoulder must correspond to the first and the second stage, respectively, and the peak observed at 853 K to the third stage.

The total weight loss for terbium formate was less than that expected to give terbium oxide, Tb_2O_3. This discrepancy between them can be ascribed to the small amount of contamination of tetraterbium heptoxide, Tb_4O_7.

Thermal decomposition of hydrous rare earth formates of Dy, Ho, Er, Tm, Yb and Lu [Table 2]

The dehydration reaction of these salts occurred in the temperature range of 340–420 K, which has been described in previous papers [18,19].

After the dehydration, an exothermic peak was observed in the DTA curves of Dy, Ho and Er formates, while the peak did not appear in those of Tm, Yb and Lu formates. This peak was attributed to the recrystallization of amorphous formate anhydride [19] (Fig. 1).

The thermal decomposition of these compounds except for $Dy(HCO_2)_3$, was very similar to each other. The thermal behaviour of $Dy(HCO_2)_3$ was similar to those of Ce, Pr, Nd, Sm, Eu and Gd formates and the decomposition proceeded through two stages

$$2\ Dy(HCO_2)_3 \rightarrow 3\ H_2 + 2\ CO_2 + 3\ CO + Dy_2O_2 \cdot CO_3$$

$$Dy_2O_2 \cdot CO_3 \rightarrow Dy_2O_3 + CO_2$$

The intermediate $Dy_2O_2 \cdot CO_3$ was identified as type I by its IR spectrum [17].

The formates of Ho, Er, Tm, Yb and Lu melted during decomposition and their decomposition processes consisted of three stages which corresponded to the formation of oxyformate, oxycarbonate and oxide [19–25].

For the decomposition of holmium formate, the second stage could not be confirmed distinctly, but the discontinuous point on the TG curve observed at 648 K suggested the formation of oxyformate. Three endothermic peaks appeared in the DTA curve. The first peak (642 K) seems to consist of two overlapping peaks corresponding to melting and the first stage. The second small peak at 647 K corresponds to the second stage, and the last, slight and broad one at around 823 K to the third decomposition stage.

TG and DTA curves for erbium formate were similar to those of yttrium formate [18] and the decomposition process took place in three stages. In the DTA curve, two endothermic peaks were observed at 593 and 625 K. The former and large peak has a shoulder at the high temperature side, and this peak and the shoulder corresponds to the melting and the first stage, respectively. The latter small peak corresponds to the second stage of the decomposition. Although the third stage proceeded very slowly without any clear endotherm, the weight loss value for this stage was in good agreement

with that expected for the formation of Er_2O_3.

The thermal behaviour of Tm, Yb and Lu formates were similar to each other. Three distinct endothermic peaks corresponding to melting, the first stage and the second stage of decomposition were observed in their DTA curves. The third stage of these compounds proceeded so slowly that any distinct endotherm was not recognized.

Intermediate oxycarbonates of Ho, Er, Tm, Yb and Lu formates were identified as type I by their IR spectra [17].

The ratio of CO_2 to CO evolved in the decomposition

The main gaseous products were H_2, CO and CO_2, and their proportions varied with each decomposition stage. These main gases contained a small amount of CH_4 and other organic compounds which were probably formed by a secondary reaction of the main gaseous products [26].

The stoichiometry of the overall decomposition of rare earth formates suggests that the reasonable ratio of CO_2 to CO is approximately 1 : 1. Contrary to expectation, the experimental value of the ratio of CO_2 to CO is larger than unity (Fig. 4), which must be attributed to the disproportionation of carbon monoxide. Figure 4 shows that the value of the ratio of CO_2 to CO is highest for cerium formate, second highest for terbium formate and the value decreases from terbium to lutetium formate. The variational tendency of the value was similar to that of the catalytic activity of the rare earth oxides in the oxidation of butane [27].

This finding suggests that the disproportionation of carbon monoxide occurred catalytically by the solid decomposition product which contained rare earth oxide as a main component.

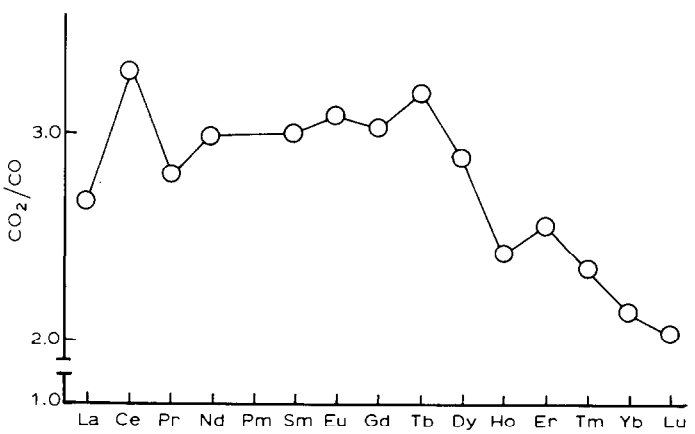

Fig. 4. The ratio of CO_2 to CO evolved in the decomposition of rare earth formates.

The relative thermal stability of rare earth formates

The initial decomposition temperature, T_i, at which evolution of gaseous products begins, can be used as a measure of the relative thermal stability of these rare earth metal formates. Figure 5 shows the relation between the ionic radii of the rare earth metallic ion and T_i. The T_i value for lanthanum to europium formate, except for cerium formate, tends to decrease slowly and decreases remarkably from gadolinium to lutetium formate. The decrease of the thermal stability of these salts must be related to their crystal structure.

It has been known that the crystal structures of anhydrous rare earth formates are all rhombohedral isostructures [28–32]. The *d* values obtained from the powder diffraction patterns are in agreement with those reported previously.

Turcotte et al. [4] have shown that the cell edge for the anhydrous rare earth formates became shortened with decrease of cation radius and the contraction of cell edge caused an increase in the rhombohedral angle. They have also suggested that the distortion of the structure which increased with increase in the rhombohedral angle, seemed to cause a different structure for the anhydrous ytterbium and lutetium formates. However, no obvious difference in their X-ray diffraction patterns could be observed in this study. But, the decrease of thermal stability of the rare earth metal formate with decreasing cationic radius is not contradictory to their suggestion.

No complete interpretation has been formulated about the anomalous behaviour of cerium formate, but the thermal unstability of cerium oxalate

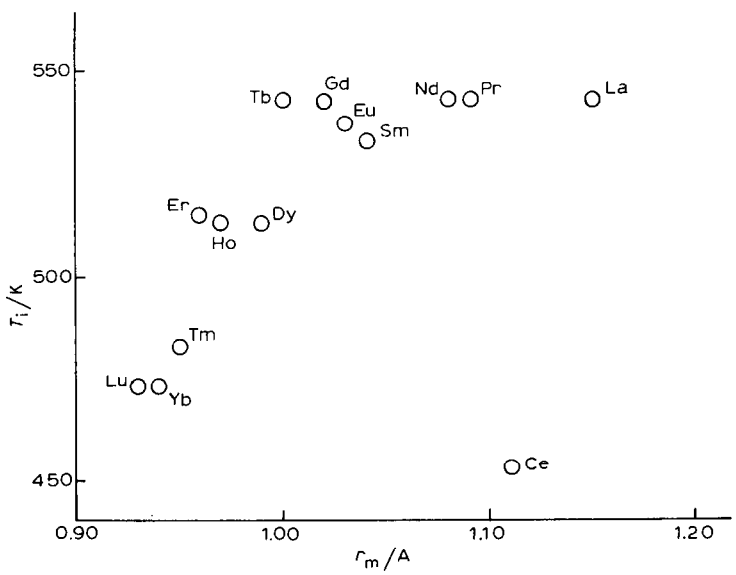

Fig. 5. Relation between T_i and ionic radii.

[33–35], malonate and succinate [36] have also been reported. These findings may be related to the smallest value of the fourth ionization potential of the cerium (III) ion as Glasner and Steinberg have suggested [34].

Kinetics of decomposition

The kinetics of the first stage of the decomposition was studied by static and dynamic methods.

Ordinarily the rate of the thermal decomposition of a solid is expressed by

$$\frac{d\alpha}{dt} = Z \exp\left(\frac{-E}{RT}\right) F(\alpha) \tag{3}$$

where t is the time, α is the fraction decomposed, Z is the pre-exponential factor, E is the activation energy, R is the gas constant, T is the temperature in degrees Kelvin, and $F(\alpha)$ is a function dependent on the mechanism

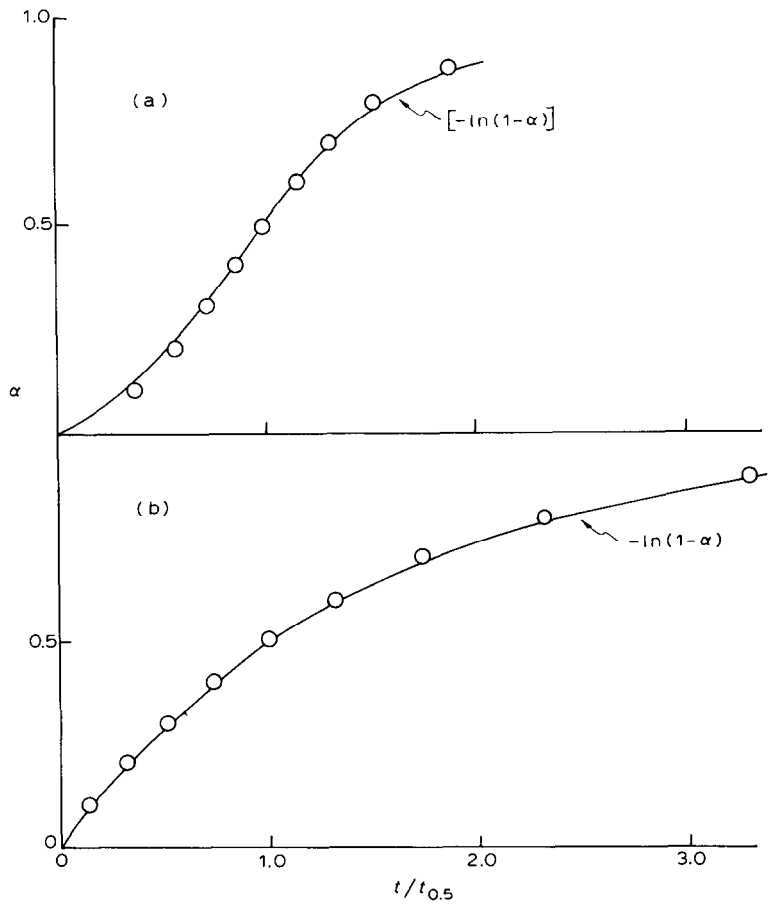

Fig. 6. Plot of α vs. $t/t_{0.5}$ for (a) $La(HCO_2)_3$ heated at 668 K and (b) $Er(HCO_2)_3$ heated at 578 K.

TABLE 3

Kinetic parameters of the thermal decomposition of rare earth formate anhydrides, $Ln(HCO_2)_3$

Ln	T (K)	E (kJ mole^{-1})	Z (sec^{-1})
La	543–683	131.8	2.0×10^{8}
Ce	453–663	87.8	6.1×10^{4}
Pr	553–713	138.5	1.2×10^{8}
Nd	533–703	112.9	1.7×10^{7}
Sm	523–693	123.8	2.0×10^{7}
Eu	537–725	127.6	6.4×10^{7}
Gd	543–693	110.9	2.5×10^{6}
Tb	543–688	108.4	1.5×10^{6}
Dy	513–673	102.5	1.1×10^{6}
Ho	513–648	146.0	1.2×10^{10}
Er	523–623	138.9	1.5×10^{10}
Tm	483–633	131.8	1.2×10^{10}
Yb	473–628	110.5	4.0×10^{7}
Lu	473–635	99.2	2.8×10^{6}

controlling the reaction [37,38]. For a linear heating rate of, say v deg min^{-1}, the rate is given by eqn. (4)

$$\left(\frac{d\alpha}{dT}\right)v = Z\exp\left(\frac{-E}{RT}\right)F(\alpha) \tag{4}$$

In this study, the kinetic parameters such as activation energy and pre-exponential factor were determined by Ozawa's method [39,40] which was a dynamic method under elevating temperature. On the other hand, $F(\alpha)$ was determined isothermally by the method of Sharp et al. [37].

Figure 6 shows the α vs. $t/t_{0.5}$ curves for $La(HCO_2)_3$ at 668 K and for $Er(HCO_2)_3$ at 578 K, where $t_{0.5}$ is the time when α has a value of 0.5. When $F(\alpha)$ was assumed A_2, the best fit between the observed and calculated curves was obtained for $La(HCO_2)_3$. $F(\alpha)$ for the first stage of decomposition of the other compounds were determined. Consequently, the most probable kinetic equation for the first main decomposition stage for lanthanum to dysprosium formate was found to be A_2, $d\alpha/dt = k(1-\alpha)[-\ln(1-\alpha)]^{1/2}$ (random nucleation reaction which is called Avrami-type reaction) [37,38,41,42] and F_1, $d\alpha/dt = k(1-\alpha)$ (first-order reaction) for holmium to lutetium formate which melted during the main stage of the decomposition. These results are summarized in Table 3.

ACKNOWLEDGEMENT

The author wishes to thank Prof. Y. Yamamoto of Hiroshima University, for his valuable advice.

REFERENCES

1 M.N. Ambroghii and Y.A. Osipova, Russ. J. Inorg. Chem., 3 (1958) 157.
2 V.E. Plyushchev, L.P. Shklover and T.A. Trushina, Russ. J. Inorg. Chem., 9 (1964) 1461.
3 V.E. Plyushchev, L.P. Shklover, L.M. Shklńikova, G.P. Kuzunetsova and T.A. Trushina, J. Gen. Chem. USSR., 35 (1965) 1781.
4 R.P. Turcotte, J.M. Haschke, M.S. Jenkins and L. Eyring, J. Solid State Chem., 2 (1970) 593.
5 C.V. Kavedia and H.B. Mathur, Indian J. Chem., 8 (1970) 638.
6 M.D. Taylor and R. Panayappan, J. Therm. Anal., 6 (1974) 673.
7 M. Dabkowska, Ann. Univ. Marie Curie-Sklodowska, Sect. AA, 29–30 (1975) 223, 241.
8 M. Dabkowska, Ann. Univ. Marie Curie-Sklodowska, Sect. AA, 31–32, (1980) 111.
9 Y. Masuda and S. Shishido, J. Inorg. Nucl. Chem., 42 (1980) 299.
10 J.R. Ferraro and M. Becker, J. Inorg. Nucl. Chem., 32 (1970) 1495.
11 F.L. Carter, F. von Batchelder, J.F. Murray and P.H. Klein, in P.E. Field (Ed.), Proc. 9th Rare Earth Res. Conf., 1971, Vol. II, Virginia Polytechnic Institute and State University, Blacksburg, VA, p. 752; Chem. Abstr., 76 (1972) 118570h.
12 J.T.M. de Hosson, J. Inorg. Nucl. Chem., 37 (1975) 2350.
13 J.T.M. de Hosson, J.P.M. Mass and M.P. Groenewege, Spectrochim. Acta, Part A, 32 (1976) 1155.
14 V.B. Kartha and T.S. Sugandhi, Indian J. Phys., 50 (1976) 115.
15 O.D. Saralide, L.P. Shklover, K.I. Petrov and V.E. Plyushchev, J. Struct. Chem. USSR, 8 (1967) 45.
16 C.J.H. Schutle and K. Buijs, Spectrochim. Acta, 20 (1964) 187.
17 R.P. Turcotte, J.O. Sawyer and L. Eyring, Inorg. Chem., 8 (1969) 238.
18 Y. Masuda, Thermochim. Acta, 53 (1982) 215.
19 Y. Masuda, Thermochim. Acta, 60 (1983) 203.
20 V.B. Glushkova and A.G. Boganov, Izv. Akad. Nauk USSR Ser. Khim., 7 (1965) 1131.
21 J.A. Goldsmith and S.D. Ross, Spectrochim. Acta, Part A, 23 (1967) 1090.
22 W.B. White and V.G. Keramidas, Spectrochim. Acta, Part A, 28 (1972) 501.
23 N.T. McDevitt and W.L. Baum, Spectrochim. Acta, Part A, 20 (1964) 799.
24 O. Kammori, N. Yamaguchi and K. Sato, Bunseki Kagaku, 16 (1967) 1050.
25 F. Petru and A. Muck, Z. Chem., 6 (1966) 386.
26 S. Shishido and Y. Masuda, Nippon Kagaku Kaishi, (1976) 66.
27 T. Hattori, J. Inoko and Y. Murakami, J. Catal., 42 (1976) 60.
28 A. Pabst, J. Chem. Phys., 11 (1943) 145.
29 I. Mayer, M. Steinberg, F. Feigenblatt and A. Glasner, J. Phys. Chem., 66 (1962) 1737.
30 V.E. Plyushchev, L.P. Shklover, L.M. Shklńikova, G.P. Kuznetsova and G.V. Nadezhdina, Dokl. Akad. Nauk USSR, 160 (1965) 366.
31 V.E. Plyushchev, L.P. Shklover and L.M. Shklńikova, J. Struct. Chem. USSR, 7 (1966) 687.
32 A. Pabst, Can. Mineral., 16 (1978) 437.
33 W.W. Wendlandt, Anal. Chem., 30 (1958) 58.
34 A. Glasner and M. Steinberg, J. Inorg. Nucl. Chem., 22 (1961) 39.
35 V.V.S. Rao, R.V.G. Rao and A.B. Biswas, J. Inorg. Nucl. Chem., 27 (1965) 2525.
36 B.S. Azikov and V.V.S. Brennikov, Russ. J. Inorg. Chem., 12 (1967) 228.
37 J.M. Sharp, G.W. Brindley and B.N.N. Achar, J. Am. Ceram. Soc., 49 (1966) 379.
38 K. Heide, W. Holand, H. Golker, K. Say, B. Muller and R. Saur, Thermochim. Acta, 13 (1975) 365.
39 T. Ozawa, Bull. Chem. Soc. Jpn., 38 (1965) 188.
40 T. Ozawa, J. Therm. Anal., 2 (1970) 301.
41 S.F. Hulbert, J. Br. Ceram. Soc., 6 (1969) 11.
42 M. Avrami, J. Chem. Phys., 7 (1939) 177; 8 (1940) 212; 9 (1941) 177.